Cell Biochem Biophys (2011) 61:585–594
DOI 10.1007/s12013-011-9241-1

ORIGINAL PAPER

Background K_{2P} Channels KCNK3/9/15 Limit the Budding of Cell Membrane-derived Vesicles

Daniel Tsung-Ning Huang · Naiwen Chi · Shiou-Ching Chen · Ting-Ying Lee · Kate Hsu

Published online: 15 July 2011

Abstract The main function of background two-pore potassium (K_{2P}) channels KCNK3/9/15 is to stabilize the cell membrane potential. We previously observed that membrane potential depolarization enhances the release of HIV-1 viruses. Because membrane polarization affects the biomembrane directly, here we examined the effects of KCNK3/9/15 on the budding of nonviral vesicles. We found that depolarization by knocking down endogenous KCNK3/9/15 promoted secretion of cell-derived vesicles. We further used Vpu (an antagonist of KCNK3) as a model for the in vivo study of depolarization-stimulated secretion. Vpu is a HIV-1-encoded, ion channel-like protein (viroporin) capable of enhancing virus release and depolarizing the cell membrane potential. We found that Vpu could also promote nonviral vesicle release, perhaps through a similar mechanism that Vpu utilizes to promote viral particle release. Notably, T cells expressing Vpu alone became pathologically low in intracellular K^+ and insensitive to extracellular K^+ or membrane potential stimulation. In contrast, heterologous expression of KCNK3 in T cells stabilized the cell potentials by maintaining intracellular K^+. We thus concluded that KCNK3/9/15 expression limits membrane depolarization and depolarization-induced secretion at least in part by maintaining intracellular K^+.

Keywords KCNK3/9/15 (TASK-1/3/5) channels · Intracellular K^+ content · Depolarization · HIV-1 Vpu · Microvesicles · Exosomes

Introduction

Vesicle secretion is an essential step for many physiological and pathophysiological processes. By releasing specific, submicron-sized vesicles, cells communicate or cross-talk with other cells and the surrounding microenvironment/systems. These cell-derived exovesicles are generated from intracellular compartments or the plasma membrane through a series of fusion and fission events. Although the origins/functions of these cell-derived exovesicles are various, their fundamental biophysical properties (e.g. fusogenicity) are similar. Most exovesicles have the capability to fuse with target cells in order to deliver cargo and transmit information. For example, the exovesicles secreted by mature dendritic cells (DCs), a type of antigen-presenting cells (APCs), bear antigen-loaded MHC molecules. When these exovesicles fuse with immature DCs, the antigens are transferred from mature to immature DCs [1]. This process could increase the number of APCs and amplify the immune responses. Besides information transmission mediated by fusion, the surface of a secreted vesicle can also serve as an antigen/biomarker-loaded presentation platform for various purposes [2]. This is best illustrated with the many types of tumor cell-derived microvesicles and exosomes. The tumor antigen-loaded exovesicles usually function to suppress a wide spectrum of

Daniel Tsung-Ning Huang and Naiwen Chi contributed equally.

D. T.-N. Huang
Department of Pediatrics, Mackay Memorial Hospital, Tamsui 251, Taiwan

N. Chi · S.-C. Chen · T.-Y. Lee · K. Hsu (✉)
Department of Medical Research, Mackay Memorial Hospital, 45 Min-Sheng Road, Research Building 616, Tamsui 251, Taiwan
e-mail: khsu1@ms1.mmh.org.tw

Present Address:
N. Chi
Bertec Enterprise Co., Ltd, Taipei, Taiwan

immune responses, but some of them secreted under stress could also counterintuitively activate the immunity [2–7]. In recent years, our understanding for the compositions and functions of cell-secreted vesicles has grown exponentially [2, 8, 9]. This report explores a lesser known aspect about the physical mechanism of vesicle biogenesis.

A universal, key regulator for membrane fusion/fission is the Ca^{2+} transient [10]. Ca^{2+} fluxes affect many factors in the exocytic machinery, such as small GTPases [9]. Another universal regulator is membrane potential stability, which is largely contributed by background K^+ channels [11, 12]. Many background K^+ channels, known as two-pore K^+ (K_{2P}) channels, share a unique two-pore (P) and four-transmembrane (2P/4TM) configuration per channel subunit. The K_{2P} (KCNK) channel family is extensively distributed in eukaryotes, and can be further divided into six subfamilies (TWIK, TREK/TRAAK, TASK, THIK, TALK, and TRESK) based on their primary sequence homology and channel properties [11]. Compared to other potassium channel families, K_{2P} channels play fundamental physiological functions, such as maintenance of membrane potential stability and regulation of cellular excitability, and are thus considered to have evolved earlier than the other K^+ channel families [11].

In particular, KCNK3 channels have been shown to reduce HIV-1 virus release [13]. We previously found that KCNK3 (also known as TASK-1) can interact destructively with HIV-1 Vpu, which is a channel-like protein [14, 15] and is capable of enhancing virus secretion [13, 16–18]. Ion channels or channel-like proteins encoded by viruses are collectively called viroporins [14]. The functions of viroporins by and large remain unclear [14, 15]. Interestingly, besides HIV-1 Vpu, murine hepatitis virus E protein and SARS coronavirus 3a protein are also viroporins capable of accelerating virus release [19–21]. However, the mechanistic links between their viroporin activities and their abilities to promote viral egress are not clear, either.

HIV-1 Vpu bears a single transmembrane domain, and may form homo-oligomers [22] and/or hetero-oligomers with host channel subunits like KCNK3 [13]. Vpu has a tremendous ability to interact with a wide range of host proteins [13, 23–29], including KCNK3 (also known as TASK-1), and to modify or destroy their normal physiological functions [13, 30, 31]. In mammalian heterologous expression systems, KCNK3 channel activities are diminished upon Vpu co-expression, whereas Vpu-mediated viral release is suppressed by KCNK3 channel activities [13]. When Vpu is expressed alone in primary T cells, it could behave like KCNK3/9/15 siRNA that reduces endogenous KCNK3/9/15 expression and depolarizes the cell membrane potential ($\Delta\psi$) [16]. Notably, the efficiency of Vpu-assisted HIV-1 release is directly correlated with the degree of membrane potential depolarization [16]. Indeed, membrane potential stability contributed by KCNK3 channels is detrimental to Vpu-mediated virus release [16].

The mechanism of Vpu-mediated virus release and the cellular mechanism of depolarization-stimulated exocytosis are similar in the aspect that they both modulate the stability of cell membrane potential. As a proof of concept, the first aim of this study was to identify the role of KCNK3/9/15 (TASK1/3/5) channels during the exocytosis process. We previously demonstrated that depolarization by KCNK3/9/15 knockdown could accelerate HIV-1 viral release [16]. Here we found that membrane depolarization by KCNK3/9/15 siRNA or by Vpu also promoted the release of cell-derived, nonviral vesicles. Some of these cell-derived exovesicles were exosomes, enriched with the lipid second messenger—ceramide. To further dissect the nature of depolarization-stimulated secretion in vivo, we measured intracellular K^+ (K^+_{in}) in Vpu+ cells, and found it to be depleted to a pathologically low level. Reduction of intracellular K^+ drives membrane potential depolarization. In contrast, heterologous expression of KCNK3 channels in primary T cells maintained K^+_{in}, thereby reinforcing membrane polarization and suppressing depolarization-stimulated exocytosis. Our results identify the $\Delta\psi$-modulatory function of KCNK3/9/15 channels and Vpu viroporin in the exocytosis process.

Materials & Methods

Plasmids and siRNA

The plasmids for GFP (pCGI) and Vpu (pCCI-Vpu) were described previously [13]. CGI (GFPIRS) and CCI are bicistronic vectors carrying reporter genes—GFP and CFP, respectively [32, 33]. To depolarize the cell membrane potentials, endogenous K_{2P} channels were knocked down by the KCNK3/9/15 siRNA described previously [16]. The knockdown efficiency of this KCNK3/9/15 siRNA was validated using siRNA-transfected HEK-293 cells by RT-PCR. The KCNK3-specific forward and reverse primers for PCR are 5′-CATCGGCTACGGGCACGCGGCAC-3′ (KCNK3T407f) and 5′-GATGACCGTGAGGCCCG TAAGGATGTAG-3′ (KCNK3T833r).

Cells and Transfection

HeLa cells were maintained in Eagle's minimum essential medium (EMEM) supplemented with 1X non-essential amino acids, 10% fetal bovine serum (FBS) and penicillin–streptomycin. HEK-293 were maintained in Dulbecco's modified Eagle's medium (DMEM) containing the same FBS and antibiotics. Jurkat and K562 cells were maintained

in RPMI media containing the same FBS and antibiotics. For primary cells, PBMC were obtained from healthy donors and maintained in RPMI containing 10% fetal calf serum (FCS), followed by 2–3 days of phytohemagglutinin and interleukin-2 activation and CD4+ cell isolation by negative selection [34]. In the secretion experiments, cells were cultured in exosome-free media. The exosomes in FBS or FCS were removed by overnight ultracentrifugation at 100,000×*g*, 4°C, followed by 0.22-μm filtration. For membrane potential depolarization, KCNK3/9/15 or the control siRNA, each with pCGI (a GFP-reporter plasmid), was transfected into cultured cells using LipofectAMINE PLUS (Invitrogen, Carlsbad, CA, USA) and into primary T cells using AMAXA transfection reagents (Lonza, Walkersville, MD, USA).

Isolation of Exosomes/Microvesicles for Electron Microscopy

The reticulocyte fraction was obtained from whole blood fractionation, and then transferred to a 0.4 μm-porous insert fitted in a 6-well plate. Fresh culture media were supplemented in the space between the insert and the well. After cell culture overnight, exosomes/microvesicles secreted by the reticulocytes could be found outside the culture insert in a well. These vesicles were extracted with sucrose gradients [35]. Briefly, the culture media outside a porous insert were resuspended and diluted in PBS, and then gently layered onto a sucrose cushion, followed by ultracentrifugation at 100,000×*g* for 75 min at 4°C. After ultracentrifugation, the sucrose cushion contained exosomes was collected with a 5-mL syringe fitted with an 18-G needle. To wash and concentrate these vesicles, this sucrose fraction was centrifuged again at 100,000×*g* for 75 min at 4°C, and then resuspended in 50–100 μL of PBS [36].

CD4+ T cells were isolated from the buffy coat of a healthy donor using Dynabeads MyPure CD4 kit (Invitrogen), followed by 2–3 days of activation. The activated CD4+ T cells were then transferred to a culture insert of 0.4-μm-porous membrane. After overnight culture, the media outside the insert were collected and subjected to vesicle isolation.

Preparation of Exosomes/Microvesicles for Electron Microscopy

The purified exosomes/microvesicles from reticulocytes or T lymphocytes were fixed in 2% paraformaldehyde and then deposited 5–10 μL onto Formvar-carbon-coated EM grids. The grids loaded with the membranous particles were briefly washed with PBS and then immersed in 1% glutaraldehyde for 5 min. The grids were then extensively washed, followed by treatments of uranyl acetate for EM contrast [36–38].

TEM for CD4+ T Cells

To visualize the effects of membrane potential depolarization on budding, human CD4+ T cells were added with an equal volume of a high K^+ balanced buffer and incubated for 45 min. The control cells were incubated with an equal volume of Hank's Balanced Saline Buffer (HBSS containing 137.9 mM NaCl, 5.33 mM KCl, 0.441 mM KH_2PO_4, 4.17 mM $NaHCO_3$, 0.338 mM Na_2HPO_4, 5.56 mM glucose, and 20 mM HEPES (pH 7.5)). The composition of the high K^+ balanced buffer was modified based on the composition of HBSS to contain 140 mM K^+ instead of Na^+. This high K^+ balanced buffer has similar osmolarity as HBSS. After high K^+ treatment, the cells were fixed with an equal volume of 5% glutaraldehyde in 0.1 M cacodylate buffer, pH 7.4, and then with 1% OsO_4. The cells were washed again with 0.1 M cacodylate buffer and then subjected to gradual dehydration by increasing ethanol concentrations. For co-polymerization, the dehydrated cells were pelleted and gradually embedded in Spurrs' resin. The resin blocks containing cell pellets were thin-sectioned onto grids, and the sections were further stained with uranyl acetate and lead citrate for EM contrast. Electron microscopy for T cells and vesicles was performed by JEOL JEM-1200EXII.

TMA-DPH Assay for Secretion Quantitation

Cultured cells or primary cells were plated on cell culture inserts of 0.4-μm-porous membrane (6-well format) for at least a day. For some experiments, 1 day after plating, the cells were transfected with siRNA and/or plasmids on the inserts, and incubated for 24–30 h to allow gene expression. At t_0 on the day of experimentation, the inserts, each layered with at least 10^6 cells, were transferred to a new 6-well culture plate containing 2 ml of HBSS or a high K^+ balanced buffer. The compositions of high K^+ balanced solutions were modified based on HBSS to keep the sum of $[K^+]$ and $[Na^+]$ constant. At each time point following t_0 (every 15 or 30 min), 125 μL of the buffer outside the insert in a well was retrieved and transferred to a FluoroNunc 96-well plate. The samples collected at each time point were stained with 5 μM of fluorescent lipid dye trimethylammonio-diphenylhexatriene (TMA-DPH, Invitrogen). TMA-DPH was excited at 350 nm and its fluorescence emission spectra were collected by SpectraMAX Gemini XS (Molecular Devices). TMA-DPH emission at each time point was subtracted with its background value obtained at t_0, and was normalized with respect to the emission values of the control cells (set 100%).

Exosome/Exovesicle Characterization by Flow Cytometry

The culture media from GFP/Vpu-transfected K562 cells were pooled and subjected to sequential centrifugation and ultracentrifugation at 4°C for exovesicles collection. The exovesicles were labeled with 4.8 μM BODIPY TR C_5-ceramide (Invitrogen) at 37°C for 30 min, followed by PBS wash. The labeled vesicles were then incubated with 10 μL of aldehyde/sulfate latex beads (Invitrogen) at 25°C for 15 min; the mixture was further diluted in 1 mL of PBS for 1 h. Lastly, the free aldehyde/sulfate groups of the beads were saturated in 100 mM glycine/PBS for 30 min, and washed twice with PBS containing 1% FCS. The expression of reporter gene GFP was assessed by the FL1 channel of a FACSCalibur flow cytometer (BD Biosciences), and ceramide labeling was assessed by the red fluorescence (FL2) channel.

Measuring Intracellular K^+ Concentrations $[K^+]_{in}$ by PBFI Flow Cytometry

IL-2-activated human CD4+ T cells were transiently transfected with GFP, Vpu/GFP, or KCNK3/GFP [16]. To assess their intracellular potassium concentrations, on day 1 post-transfection, the cells were incubated in 5 μM of K^+-specific fluorescent indicator PBFI-AM (Invitrogen) for 20 min at 37°C. The K_d of PBFI were reported 5.1 mM in a Na^+-free milieu and 44 mM in a solution of 135 mM of Na^+ and K^+ in combine [39]. Thus, the changes of intracellular K^+ concentrations can be reliably assessed by PBFI. For calibration, a portion of the PBFI-loaded cells were incubated with 2–4 μM valinomycin in balanced salt solutions containing different concentrations of K^+. On a FACSCalibur, the green fluorescent cells were gated at FL1, and their PBFI intensities were collected at the FL5 channel (excitation/emission: 350/500 nm) [40, 41]. Membrane potentials were calculated with the measured $[K^+]_{in}$ according to the Nernst equation.

Results

Characterization of Exovesicle Release by TMA-DPH Staining

We hypothesized that membrane potential depolarization may affect the budding efficiency of nonviral vesicles. Based on the Nernst equation, the negative cell membrane potential is largely resulted from the high concentration of K^+ inside a cell ($[K^+]_{in}$) and the relatively low extracellular concentration of K^+ ($[K^+]_{out}$: about 4–8 mM for most tissues). Therefore, depolarization can be achieved by reducing the differences between $[K^+]_{in}$ and $[K^+]_{out}$. Under a transmission electron microscope (TEM), the vesicles released from human CD4+ T cells incubated in a high-K^+ (73 mM K^+) exhibited spherical shapes and sizes (44–172 nm in diameter; Fig. 1a). These exovesicles were not morphologically very different from those originated from the cells incubated in 5 mM K^+. But it was not possible to accurately determine whether there were more exovesicles released from the depolarized cells by TEM.

We quantified exovesicle release by fluorescence labeling of these exovesicles with a fluorescent lipid probe—TMA-DPH. TMA-DPH primarily anchors onto the positively-charged polar head groups of phospholipids [42]. Upon binding to lipid, TMA-DPH emits fluorescence; this probe does not fluoresce in aqueous solutions [43]. Because TMA-DPH fast and readily partitions between lipid and water, it has been used for labeling of exocytosed membrane [44, 45]. We validated this TMA-DPH-based, quantitative method with Jurkat cells (a cell line of T lymphocytes), and found an excellent linear correlation between the amount of TMA-DPH labeling and the quantities of cells or cell membrane (Fig. 1b).

To distinguish exovesicles from large cell debris or shed membrane fragments, we cultured cells on 0.4-μm-porous inserts. These inserts were fitted onto culture wells, and functioned as "sieves" that only allowed particles with diameters smaller than 0.4 μm to pass through. A substantial portion of cell debris and membrane fragments remained inside the inserts because of their generally larger sizes or buoyancy. At the beginning of a vesicle quantitation experiment (t_0), the culture medium or balanced buffer outside the insert was replaced with a fresh one. For every 15 or 30 min, an aliquot (usually 1/20) of the buffer outside the insert was retrieved for TMA-DPH labeling. We observed that the fluorescence emission of TMA-DPH was significantly higher at t_{30min} than at t_0 (Fig. 1c), indicating that some exovesicles/lipids had diffused from inside to outside the culture insert within the 30-min interval. To quantify vesicle release induced by depolarization, HeLa cells were transferred to a well filled with a high K^+ balanced buffer at t_0. Compared to the negative-control set immersed in 5 mM K^+, high K^+-induced depolarization enhanced vesicle release by ~2 folds (Fig. 1d). Similar depolarization-stimulated release has also been observed in HEK-293 cells and in activated human CD4+ T cells.

We also tested whether depolarization triggered by knocking down major background K_{2P} channels could promote vesicle release. The endogenous background K_{2P} channels were knocked down with KCNK3/9/15 siRNA. This siRNA was previously designed to effectively reduce the expression of KCNK3 channels, and has been shown to substantially depolarize the resting membrane potentials of primary T cells, HEK-293 and HeLa cells [16]. Because

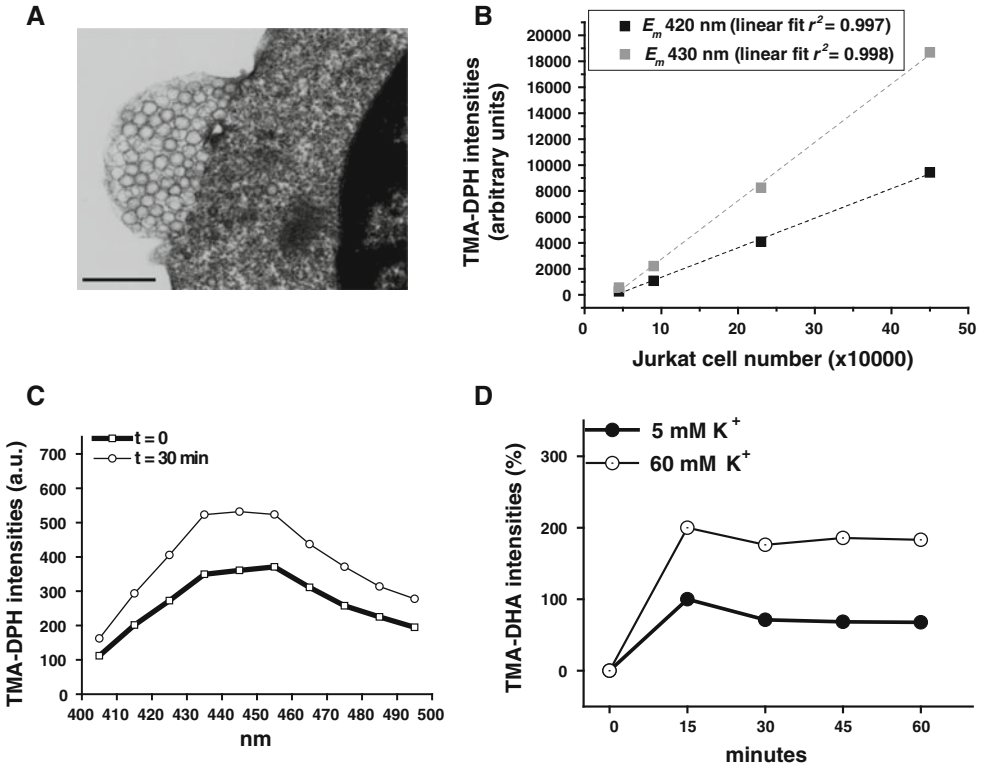

Fig. 1 Membrane potential depolarization by immersing cells in a high-K^+ buffer promoted vesicle release. **a** TEM showed vesicle budding from an activated human CD4+ T lymphocyte incubated in a high-K^+ balanced buffer (extracellular $[K^+] = 73$ mM). After 45 min of incubation in high K^+, the cells were fixed with an equal volume of 5% glutaraldehyde, followed by OsO_4 fixation. The cells were then gently spun down in a microcentrifuge tube for embedding and copolymerization. Thin-sections of the cells in resin blocks were visualized by TEM (JEOL JEM-1200EXII). Bar = 500 nm. **b** To validate the membrane quantitation method by TMA-DPH, Jurkat cells were divided into 4 groups of different cell numbers (ranging from 4.5×10^4 to 4.5×10^5 cells per group) for TMA-DPH labeling. The labeled cells were excited at 350 nm, and their emission was collected at 420–490 nm. For each E_m wavelength tested, the fluorescence emission intensities all exhibited linear correlations with the quantities of cells or cell membrane ($r^2 > 0.99$). Shown here were the linear correlations at E_m 420 nm and 430 nm. **c** HeLa cells were plated in 6-well culture inserts of 0.4-μm-porous membrane. After 24–30 h of siRNA transfection, culture media outside the insert in each well were replaced with fresh ones, and a fraction of the sieved media (outside the culture insert in a well) were collected every 15 or 30 min for TMA-DPH labeling. As revealed by the TMA-DPH emission spectra at t_0 and t_{30} (30 min of membrane secretion), the fluorescent emission of TMA-DPH was greatly enhanced upon binding to the exocytosed membranes. The maximal emission of TMA-DPH was determined at 445 nm excitation, and the E_m at this excitation wavelength will be used for all the quantitative comparison below. **d** Membrane potential depolarization induced by a high-K^+ buffer stimulated vesicle secretion. At t_0, the culture inserts layered with HeLa cells were transferred to wells containing HBSS (5 mM K^+) or a high K^+ balanced buffer (60 mM K^+). A fraction of the buffer outside the porous inserts was retrieved at each time point for TMA-DPH staining. At the end of secretion collection, the cells on the culture inserts were resuspended and transferred to a 96-well plate for measurements of TMA-DPH fluorescence intensities. The variations of cell membrane quantities from set to set were relatively small (<5%), as compared to the changes due to high K^+ stimulation (>50% in general). The experiments have been repeatedly observed in HEK-293 cells and in IL-2-activated human CD4+ T lymphocytes

this siRNA sequence also matches homologous KCNK9 (89%) and KCNK15 (95%), it is named KCNK3/9/15 siRNA. From RT-PCR experiments, the KCNK3/9/15 siRNA reduced ~90% of KCNK3 at the transcription level in HEK-293 cells (Fig. 2a). The knockdown efficiencies for KCNK9 or KCNK15 have not been evaluated, because KCNK9 or KCNK15 mRNA was not found in the cell lines we commonly used (e.g. HEK-293 cells).

To determine the function of KCNK3 during secretion, at t_0 of a TMA-DPH experiment (usually between the 24th and the 30th hour post-transfection of the control or KCNK3 siRNA), cells on porous inserts were transferred to a new 6-well plate filled with HBSS. An aliquot of HBSS outside the insert was retrieved for TMA-DPH labeling every 15 min. We found that the cells depolarized by KCNK3/9/15 siRNA indeed secreted more vesicles than the control, non-depolarized cells (Fig. 3b). Both means of $\Delta\psi$ reduction ((1) high K^+_{out} and (2) KCNK3/9/15 siRNA) enhanced vesicle secretion (Figs. 1, 2).

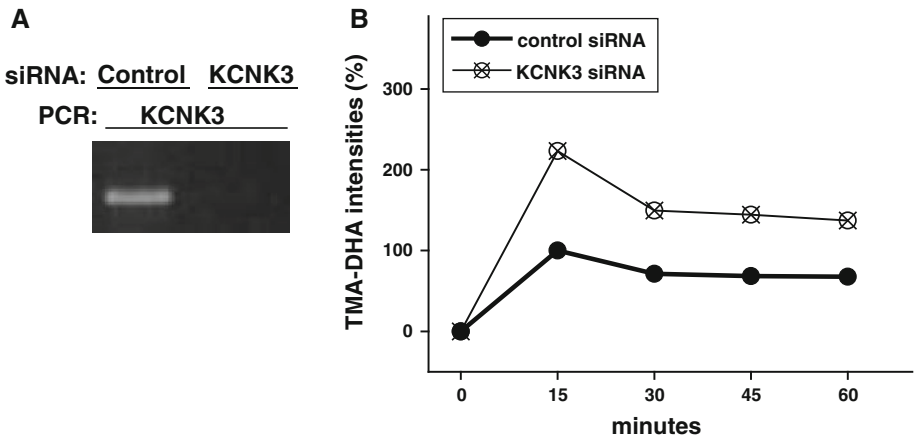

Fig. 2 Membrane potential depolarization by knocking down endogenous KCNK3/9/15 channels promoted the release of membranous particles. **a** To validate the knockdown efficiencies of the KCNK3/9/15 siRNA, HEK-293 cells were transiently transfected with the KCNK3/9/15 siRNA or the control siRNA for 2 days, followed by extraction of total RNA and reverse transcription. The remaining expression of KCNK3 after knockdown was amplified by PCR and quantitatively compared by ImageJ. **b** Depolarization by KCNK3/9/15 knockdown stimulated secretion from HeLa cells. The experiments have also been repeatedly observed in HEK-293 cells and in IL-2-activated human CD4+ T lymphocytes

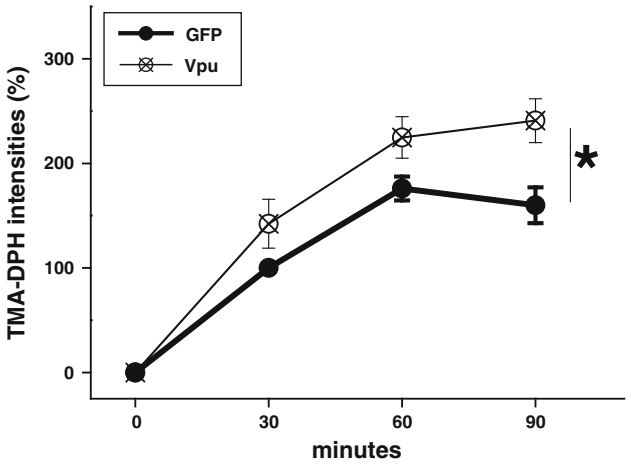

Fig. 3 Vpu promoted secretion of nonviral vesicles. IL-2-activated human CD4+ T lymphocytes were transfected with bicistronic plasmids pCGI (containing GFP) alone, or together with pCCI-Vpu, using AMAXA transfection reagents. After 5–8 h of transient transfection, the cells were transferred to culture inserts fitted in a 6-well plate. Gene expression was monitored by % green or cyan fluorescence at the 18th–24th hour post-transfection, and 30-60% fluorescent cells were usually observed. At t_0 on the day of experimentation, the inserts loaded with the transfected T cells were transferred to a new 6-well culture plate filled with HBSS. At each time point (30-min intervals), a fraction of HBSS outside the insert was retrieved for TMA-DPH staining. Vpu+ cells (*hallow circle symbols*) secreted significantly more membranous particles than GFP+ cells (*solid circle symbols*). The data were averaged from 5 independent experiments. $*P < 0.05$ deemed significant

Release of Nonviral Vesicles Promoted by HIV-1 Vpu

As a proof of principle, we also examined if Vpu, a viroporin of HIV-1 capable of depolarizing the cell membrane potential, could stimulate nonviral vesicle release. Heterologous expression of Vpu in primary CD4+ T cells and in common cultured cells can depolarize the cell membrane potentials by 5-20 mV [13]. Here, IL-2-activated human CD4+ T cells were transfected with vpu-GFP or GFP (control) plasmids on 0.4 μm-porous culture inserts. At t_0 of a secretion experiment, the culture inserts loaded with transfected cells were transferred to new wells filled with HBSS. For every 30 min, an aliquot of HBSS outside the inserts was retrieved for TMA-DPH labeling. We observed ~50% more TMA-DPH-labeled membranes due to the expression of depolarizing Vpu (Fig. 3). The differences between Vpu+ and GFP+ groups were significant ($*P < 0.05$ from 5 independent experiments), albeit that the increase of secretion by Vpu (~50% in Fig. 3) was smaller than that by KCNK3/9/15 siRNA or by high K^+_{out} (~2 folds in Figs. 1, 2).

Because TMA-DPH also stains lipids and membranous debris, we also checked the content of secretion at the end of a typical TMA-DPH experiment (as in Fig. 3) using another TEM technique. The exocytosed particles outside the insert were isolated and concentrated by ultracentrifugation (up to 100,000×*g*). Under a TEM, the 0.4-μm-sieved, exocytosed vesicles looked like "half-deflated balloons" (Fig. 4a). Others have pointed out that these variations in EM preparation could make these submicron-sized vesicles look "cup-shaped" [8]. For confirmation and comparison, we also isolated exosomes released from human reticulocytes. The reticulocyte-derived exosomes also exhibited irregular or cup shapes (Fig. 4b), similar to those vesicles secreted from the depolarized T cells (Fig. 4a).

The sizes of these secreted vesicles were less than 200 nm in diameter and somewhat heterogeneous (Fig. 4a, b).

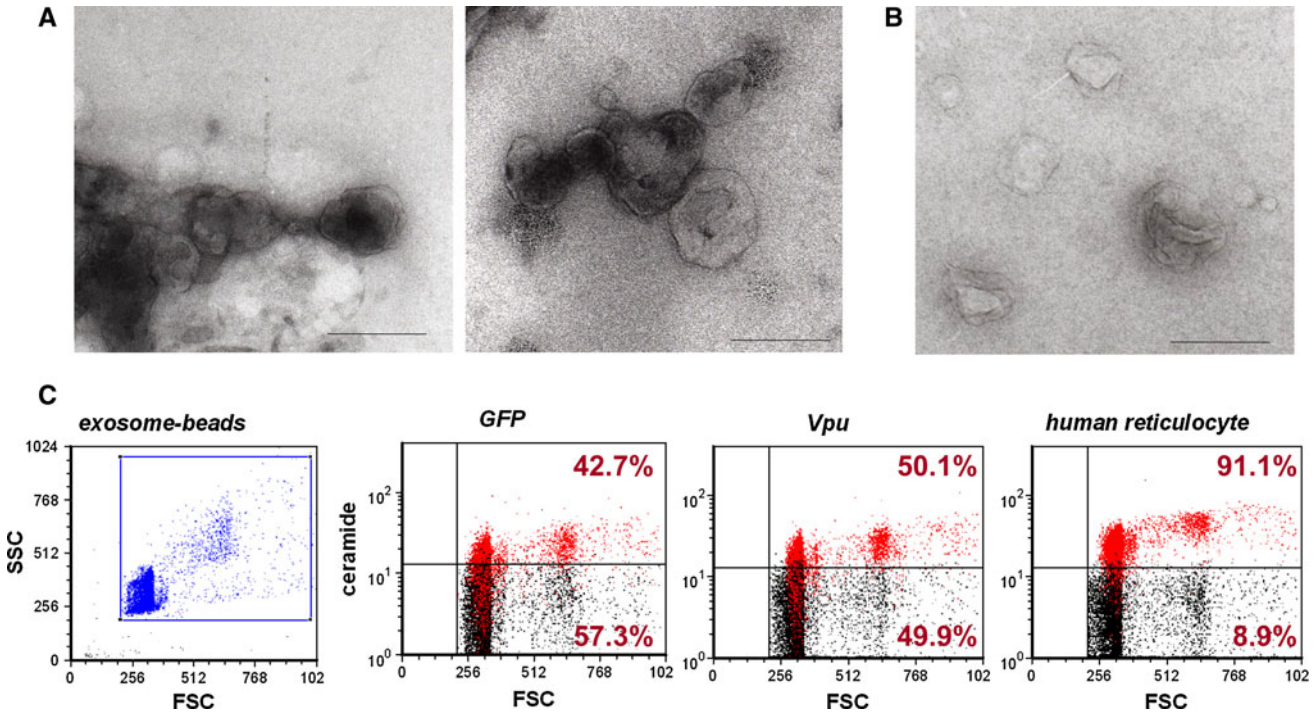

Fig. 4 The depolarization-stimulated exovesicle pool contained exosomes. Many vesicles induced by depolarization from IL-2-activated CD4+ T cells (**a**) exhibited similar morphology as the exosomes released from human reticulocytes (**b**). Depolarization was induced by knockdown of endogenous KCNK3/9/15 (**a**, *left*) or by Vpu expression (**a**, *right*). Human T cells or reticulocytes were cultured on cell culture inserts of 0.4-μm-porous membrane in a 6-well plate overnight. The culture media outside the inserts were collected to extract the secreted exosomes/vesicles. The isolated and concentrated vesicles were then fixed in 2% paraformaldehyde and deposited onto Formvar-carbon coated EM grids. The sample-loaded grids were further washed, fixed, and stained with uranyl acetate. These membranous particles were visualized by JEOL JEM-1200EXII. Bar = 200 nm. **c** A significant portion of the exovesicles were exosomes. The fluorescent probe, BODIPY TR C_5-ceramide, was used to label exosomes for flow cytometric analyses. The vesicle-coated beads were found monomeric, dimeric, and trimeric in a FSC/SSC dot plot, as gated (*left*). BODIPY TR C_5-ceramide labeling could be detected by the FL-2 channel for red fluorescence. BODIPY TR C_5-ceramide-stained exovesicles were gated in the *upper-right* quadrant of the *dot plot*. For each experimental set, the control group (unstained exovesicles) was also shown, and gated in the *lower-right* quadrant. Over 90% of the reticulocyte-derived exosomes were positively labeled by BODIPY TR C_5-ceramide. About half of the exovesicle population from the GFP/Vpu-transfected cells was exosomes

Thus, the secretion pools probably included various types of vesicles, such as exosomes (40-100 nm in diameter) [36], exosome-like vesicles (20-50 nm) [46], membrane particles (50-80 nm) [2, 47], and few microvesicles (100-1,000 nm) [48]. Despite that these exovesicles might have originated from various intracellular compartments and/or the plasma membrane, minimization of membrane potential polarization could induce their secretion. Thus, membrane depolarization is likely a general mechanism for vesicle biogenesis/release.

We further attempted to characterize these depolarization-induced exovesicles with biomarkers. In particular, we were interested in the fraction of exosomes in the secretion pool, since exosomes are biologically important and have been well characterized. We first confirmed that human reticulocyte-derived exosomes were enriched with transferrin receptor (TrnR). For convenience, we then used K562 cultured cells (of an erythroleukemic type) to generate sufficient quantities of exovesicles for this study. K562 cells were transiently transfected with GFP or GFP/Vpu, and the exovesicles secreted from these cells were concentrated by ultracentrifugation. Some of the exovesicles secreted from K562 cells also expressed transferrin receptors (TrnR), suggesting that they might be exosomes. On the other hand, not many exovesicles secreted from K562 cells or human reticulocytes expressed CD81, a tetraspanin protein and an exosome marker specific for antigen-presenting cells (data not shown). Since exosome markers are cell type-dependent, and both K562 cells and reticulocytes are not antigen-presenting cells, their exovesicles should indeed contain very little CD81. Because membrane potential depolarization should be a universal, physical mechanism for stimulation of secretion, we chose a more generalized biomarker—ceramide, to characterize these exovesicles. Ceramide is a marker for the Golgi apparatus, exosomes, and the secretory pathway for exosomes [35, 49]. We established a flow cytometry-based quantitative method for ceramide. Since the cell-derived exovesicles were too small (<200 nm in diameters) for flow cytometry, they were first labeled with BODIPY

TR C_5-ceramide, and then coated onto aldehyde/sulfate-treated latex beads. We found that most reticulocyte-derived exosomes were loaded with ceramide (91.1%, Fig. 4c). The ceramide levels were significant in ~42.7% of the exovesicles originated from GFP+ cells, and in ~50.1% of the exovesicles from GFP/Vpu+ cells (Fig. 4c). There were also populations of non-exosome vesicles in the secretion. Interestingly, Vpu expression might be able to promote exosome secretion, as it slightly increased the proportion of exosomes in the exovesicle pools.

Depolarization In Vivo Associated With Depletion of Intracellular K^+

The concentration of free K^+ ions in human plasma is ~5 mM, and the intracellular K^+ content is generally much higher [50]. We directly measured $[K^+]_{in}$ by labeling intracellular K^+ ions with a K^+-specific fluorescent indicator—PBFI. As shown in Fig. 5a, increasing the extracellular K^+ concentration forced $[K^+]_{in}$ to increase in a non-linear fashion. Noticeably, heterologous expression of Vpu alone in the activated CD4+ T cells rendered the cells to be significantly less sensitive to $[K^+]_{out}$ changes, indicating a lack of K^+ channel expression on their plasma membrane (Fig. 5a). Importantly, the intracellular K^+ content was significantly lower in Vpu+ cells (Fig. 5a). Because Vpu could form viroporins by itself or oligomerize with host channel subunits [16, 51], its disruption of normal cell electrophysiology conceivably could result in a constitutive leak of intracellular K^+ (Fig. 5).

From the Nernst equation, the changes of intracellular and extracellular K^+ concentrations directly affect the cell membrane potential. With a decrease in $[K^+]_{in}$ and insensitivity to $[K^+]_{out}$, the differences between $[K^+]_{in}$ and $[K^+]_{out}$ for Vpu+ cells were minimized, and consequently their membrane potentials were more depolarized (Fig. 5b). In contrast, KCNK3+ cells showed higher $[K^+]_{in}$ than the control cells throughout most $[K^+]_{out}$ tested (Fig. 5a), and thus their cell membrane potentials were more polarized (Fig. 5b).

Discussion

The resting membrane potentials for most cell types range from −40 to −95 mV [52], and the electric field across a biomembrane is in the order of 10^5V/cm [53]. This stored energy in a biomembrane is undoubtedly a significant energy constraint for any structural transition of the membrane. A relatively small reduction of $\Delta\psi$ (such as the induced depolarization presented here) could accelerate the rate of membrane fusion/fission and increase secretion. In this study, we demonstrated that depolarization by manipulating K^+ gradients across the cell membrane could independently promote the release of membranous particles from common cultured cell lines (i.e. HEK-293 and HeLa cells) and from activated human CD4+ T cells (Figs. 1, 2). Depolarization by heterologous expression of Vpu also stimulated the release of nonviral vesicles in primary T cells (Fig. 3). Since depolarization could lower the electrostatic repulsion on a vesicle-budding membrane [16, 53], our results suggest that the electric field across a cell membrane is an important energy barrier for vesicle biogenesis/secretion.

We identified K^+_{in} depletion as a major cause of depolarization in vivo (Fig. 5). An intracellular milieu of low

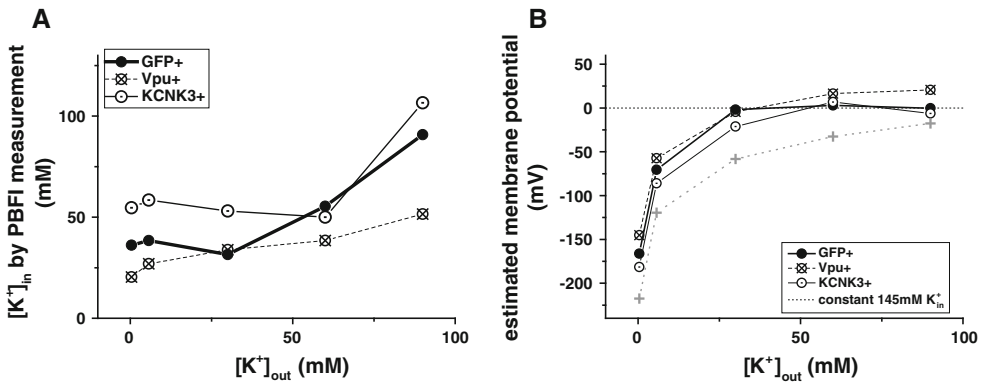

Fig. 5 Loss of intracellular K^+ in Vpu+ human T cells attributed to membrane depolarization. **a** Heterologous expression of Vpu resulted in a substantial loss of intracellular K^+ (K^+_{in}), as compared to the expression of GFP or KCNK3 in the activated T cells. K^+_{in} was labeled with fluorescent indicator PBFI, and quantitatively assessed by flow cytometry. A representative experiment is shown here. Each dot represents the measured $[K^+]_{in}$ at an extracellular K^+ concentration. **b** The cell membrane potentials at different extracellular $[K^+]$ were estimated from $\log([K^+]_{out}/[K^+]_{in})$. In physiological 5.7 mM K^+_{out}, Vpu+ cells were in average 13.2 mV more depolarized than GFP+ cells, whereas KCNK3+ cells were 15.5 mV more hyperpolarized than GFP+ cells. For comparison, if the intracellular K^+ concentration were set to be 145 mM throughout all $[K^+]_{out}$, the corresponding potentials (*cross symbols*) in theory would be more negative than the experimental data here

K^+ is favored by apoptosis [54]. Notably, Vpu can independently facilitate apoptosis [55], so Vpu-mediated apoptosis might conceivably require the viroporin activity to disrupt intracellular K^+ homeostasis and $\Delta\psi$. In comparison, heterologous expression of KCNK3 in human CD4+ T cells prevented pathological leak of K^+_{in} (Fig. 5a) and stabilized the cells at polarized potentials (Fig. 5b). Could KCNK3, an antagonist of Vpu, exert protection against apoptosis during HIV-1 infection? Liu et al. [56] have shown that membrane hyperpolarization driven by various K_{2P} channels, including KCNK3, inhibits activation of apoptosis during cell stress in cultured rat hippocampal slices. On the other hand, Lauritzen et al. [57] have shown that KCNK9 channels could result in K^+_{in} depletion and activation of apoptosis instead. Conceivably, the differences in KCNK channel activities, $\Delta\psi$ stability, and cellular regulation of KCNK expression could all influence K^+_{in} homeostasis directly, resulting in inhibition or activation of apoptosis.

During HIV-1 infection, the main retroviral structural component—Gag is required for Vpu-mediated budding of viral and pseudoviral particles [58]. However, in the absence of Gag, Vpu expression alone still contributed ~50% increase of nonviral vesicle release (Fig. 3). These data again support the depolarization model [16] that Vpu expression directly affects the physical property of a biomembrane to promote secretion.

Acknowledgments We thank Y. Lin for laboratory assistance (M.M.H.). The work was supported by an intramural grant from Mackay Memorial Hospital to K.H. and by a grant from the C.L. Chen Foundation to D.H.

References

1. Obregon, C., Rothen-Rutishauser, B., Gitahi, S. K., Gehr, P., & Nicod, L. P. (2006). Exovesicles from human activated dendritic cells fuse with resting dendritic cells, allowing them to present alloantigens. *American Journal of Pathology, 169*, 2127–2136.
2. Thery, C., Ostrowski, M., & Segura, E. (2009). Membrane vesicles as conveyors of immune responses. *Nature Reviews Immunology, 9*, 581–593.
3. Gastpar, R., Gehrmann, M., Bausero, M. A., Asea, A., Gross, C., Schroeder, J. A., et al. (2005). Heat shock protein 70 surface-positive tumor exosomes stimulate migratory and cytolytic activity of natural killer cells. *Cancer Research, 65*, 5238–5247.
4. Vega, V. L., Rodriguez-Silva, M., Frey, T., Gehrmann, M., Diaz, J. C., Steinem, C., et al. (2008). Hsp70 translocates into the plasma membrane after stress and is released into the extracellular environment in a membrane-associated form that activates macrophages. *Journal of Immunology, 180*, 4299–4307.
5. Clayton, A., Mitchell, J. P., Court, J., Mason, M. D., & Tabi, Z. (2007). Human tumor-derived exosomes selectively impair lymphocyte responses to interleukin-2. *Cancer Research, 67*, 7458–7466.
6. Clayton, A., Mitchell, J. P., Court, J., Linnane, S., Mason, M. D., & Tabi, Z. (2008). Human tumor-derived exosomes down-modulate NKG2D expression. *Journal of Immunology, 180*, 7249–7258.
7. Liu, C., Yu, S., Zinn, K., Wang, J., Zhang, L., Jia, Y., et al. (2006). Murine mammary carcinoma exosomes promote tumor growth by suppression of NK cell function. *Journal of Immunology, 176*, 1375–1385.
8. Fevrier, B., & Raposo, G. (2004). Exosomes: endosomal-derived vesicles shipping extracellular messages. *Current Opinion in Cell Biology, 16*, 415–421.
9. Simons, M., & Raposo, G. (2009). Exosomes–vesicular carriers for intercellular communication. *Current Opinion in Cell Biology, 21*, 575–581.
10. Savina, A., Furlan, M., Vidal, M., & Colombo, M. I. (2003). Exosome release is regulated by a calcium-dependent mechanism in K562 cells. *J Biol Chem, 278*, 20083–20090.
11. Enyedi, P., & Czirjak, G. (2010). Molecular background of leak K+ currents: two-pore domain potassium channels. *Physiological Reviews, 90*, 559–605.
12. Goldstein, S. A., Bockenhauer, D., O'Kelly, I., & Zilberberg, N. (2001). Potassium leak channels and the KCNK family of two-P-domain subunits. *Nature Reviews Neuroscience, 2*, 175–184.
13. Hsu, K., Seharaseyon, J., Dong, P., Bour, S., & Marban, E. (2004). Mutual functional destruction of HIV-1 Vpu and host TASK-1 channel. *Molecular Cell, 14*, 259–267.
14. Gonzalez, M. E., & Carrasco, L. (2003). Viroporins. *FEBS Letters, 552*, 28–34.
15. Fischer, W. B., & Kruger, J. (2009). Viral channel-forming proteins. *International Review of Cell and Molecular Biology, 275*, 35–63.
16. Hsu, K., Han, J., Shinlapawittayatorn, K., Deschenes, I., & Marban, E. (2010). Membrane potential depolarization as a triggering mechanism for Vpu-mediated HIV-1 release. *Biophysical Journal, 99*, 1718–1725.
17. Hsu, K. (2009). Long-chain polyunsaturated fatty acids as anti-HIV supplementation during breastfeeding. *Taiwanese Journal of Obstetrics and Gynecology, 48*, 65–68.
18. Bour, S., & Strebel, K. (2003). The HIV-1 Vpu protein: a multifunctional enhancer of viral particle release. *Microbes and Infection, 5*, 1029–1039.
19. Lu, W., Zheng, B. J., Xu, K., Schwarz, W., Du, L., Wong, C. K., et al. (2006). Severe acute respiratory syndrome-associated coronavirus 3a protein forms an ion channel and modulates virus release. *Proceedings of the National Academy of Sciences of the USA, 103*, 12540–12545.
20. Maeda, J., Maeda, A., & Makino, S. (1999). Release of coronavirus E protein in membrane vesicles from virus-infected cells and E protein-expressing cells. *Virology, 263*, 265–272.
21. Madan, V., Garcia Mde, J., Sanz, M. A., & Carrasco, L. (2005). Viroporin activity of murine hepatitis virus E protein. *FEBS Letters, 579*, 3607–3612.
22. Maldarelli, F., Chen, M. Y., Willey, R. L., & Strebel, K. (1993). Human immunodeficiency virus type 1 Vpu protein is an oligomeric type I integral membrane protein. *Journal of Virology, 67*, 5056–5061.
23. Margottin, F., Bour, S. P., Durand, H., Selig, L., Benichou, S., Richard, V., et al. (1998). A novel human WD protein, h-beta TrCp, that interacts with HIV-1 Vpu connects CD4 to the ER degradation pathway through an F-box motif. *Molecular Cell, 1*, 565–574.
24. Callahan, M. A., Handley, M. A., Lee, Y. H., Talbot, K. J., Harper, J. W., & Panganiban, A. T. (1998). Functional interaction of human immunodeficiency virus type 1 Vpu and Gag with a novel member of the tetratricopeptide repeat protein family. *Journal of Virology, 72*, 8461.

25. Hussain, A., Wesley, C., Khalid, M., Chaudhry, A., & Jameel, S. (2008). Human immunodeficiency virus type 1 Vpu protein interacts with CD74 and modulates major histocompatibility complex class II presentation. *Journal of Virology, 82*, 893–902.
26. Neil, S. J., Zang, T., & Bieniasz, P. D. (2008). Tetherin inhibits retrovirus release and is antagonized by HIV-1 Vpu. *Nature, 451*, 425–430.
27. Van Damme, N., Goff, D., Katsura, C., Jorgenson, R. L., Mitchell, R., Johnson, M. C., et al. (2008). The interferon-induced protein BST-2 restricts HIV-1 release and is downregulated from the cell surface by the viral Vpu protein. *Cell Host Microbe, 3*, 245–252.
28. Varthakavi, V., Heimann-Nichols, E., Smith, R. M., Sun, Y., Bram, R. J., Ali, S., et al. (2008). Identification of calcium-modulating cyclophilin ligand as a human host restriction to HIV-1 release overcome by Vpu. *Nature Medicine, 14*, 641–647.
29. Shah, A. H., Sowrirajan, B., Davis, Z. B., Ward, J. P., Campbell, E. M., Planelles, V., et al. (2010). Degranulation of natural killer cells following interaction with HIV-1-infected cells is hindered by downmodulation of NTB-A by Vpu. *Cell Host Microbe, 8*, 397–409.
30. Coady, M. J., Daniel, N. G., Tiganos, E., Allain, B., Friborg, J., Lapointe, J. Y., et al. (1998). Effects of Vpu expression on Xenopus oocyte membrane conductance. *Virology, 244*, 39–49.
31. Ewart, G. D., Sutherland, T., Gage, P. W., & Cox, G. B. (1996). The Vpu protein of human immunodeficiency virus type 1 forms cation-selective ion channels. *Journal of Virology, 70*, 7108–7115.
32. Johns, D. C., Nuss, H. B., & Marban, E. (1997). Suppression of neuronal and cardiac transient outward currents by viral gene transfer of dominant-negative Kv4.2 constructs. *Journal of Biological Chemistry, 272*, 31598–31603.
33. Hoppe, U. C., Johns, D. C., Marban, E., & O'Rourke, B. (1999). Manipulation of cellular excitability by cell fusion: effects of rapid introduction of transient outward K+ current on the guinea pig action potential. *Circulation Research, 84*, 964–972.
34. Zhou, Y., Zhang, H., Siliciano, J. D., & Siliciano, R. F. (2005). Kinetics of human immunodeficiency virus type 1 decay following entry into resting CD4+ T cells. *Journal of Virology, 79*, 2199–2210.
35. Laulagnier, K., Grand, D., Dujardin, A., Hamdi, S., Vincent-Schneider, H., Lankar, D., et al. (2004). PLD2 is enriched on exosomes and its activity is correlated to the release of exosomes. *FEBS Letters, 572*, 11–14.
36. Thery, C., Amigorena, S., Raposo, G. & Clayton, A. (2006) Isolation and characterization of exosomes from cell culture supernatants and biological fluids. In *Current protocols in cell biology* (p. 3.22.12). New York: Wiley.
37. Yu, X., Harris, S. L., & Levine, A. J. (2006). The regulation of exosome secretion: a novel function of the p53 protein. *Cancer Research, 66*, 4795–4801.
38. Caby, M. P., Lankar, D., Vincendeau-Scherrer, C., Raposo, G., & Bonnerot, C. (2005). Exosomal-like vesicles are present in human blood plasma. *International Immunology, 17*, 879–887.
39. Johnson, I. & Spence, M. (2010). The molecular probes handbook (11th ed.) Eugene: Invitrogen.
40. Voss, T. G., Fermin, C. D., Levy, J. A., Vigh, S., Choi, B., & Garry, R. F. (1996). Alteration of intracellular potassium and sodium concentrations correlates with induction of cytopathic effects by human immunodeficiency virus. *Journal of Virology, 70*, 5447–5454.
41. Heimlich, G., & Cidlowski, J. A. (2006). Selective role of intracellular chloride in the regulation of the intrinsic but not extrinsic pathway of apoptosis in Jurkat T-cells. *Journal of Biological Chemistry, 281*, 2232–2241.
42. Prendergast, F. G., Haugland, R. P., & Callahan, P. J. (1981). 1-[4-(Trimethylamino)phenyl]-6-phenylhexa-1,3,5-triene: Synthesis, fluorescence properties, and use as a fluorescence probe of lipid bilayers. *Biochemistry, 20*, 7333–7338.
43. Bronner, C., Landry, Y., Fonteneau, P., & Kuhry, J. G. (1986). A fluorescent hydrophobic probe used for monitoring the kinetics of exocytosis phenomena. *Biochemistry, 25*, 2149–2154.
44. Kuhry, J. G., Fonteneau, P., Duportail, G., Maechling, C., & Laustriat, G. (1983). TMA-DPH: a suitable fluorescence polarization probe for specific plasma membrane fluidity studies in intact living cells. *Cell Biophysics, 5*, 129–140.
45. Kubina, M., Lanza, F., Cazenave, J. P., Laustriat, G., & Kuhry, J. G. (1987). Parallel investigation of exocytosis kinetics and membrane fluidity changes in human platelets with the fluorescent probe, trimethylammonio-diphenylhexatriene. *Biochimica et Biophysica Acta, 901*, 138–146.
46. Hawari, F. I., Rouhani, F. N., Cui, X., Yu, Z. X., Buckley, C., Kaler, M., et al. (2004). Release of full-length 55-kDa TNF receptor 1 in exosome-like vesicles: a mechanism for generation of soluble cytokine receptors. *Proceedings of the National Academy of Sciences of the USA, 101*, 1297–1302.
47. Marzesco, A. M., Janich, P., Wilsch-Brauninger, M., Dubreuil, V., Langenfeld, K., Corbeil, D., et al. (2005). Release of extracellular membrane particles carrying the stem cell marker prominin-1 (CD133) from neural progenitors and other epithelial cells. *Journal of Cell Science, 118*, 2849–2858.
48. Heijnen, H. F., Schiel, A. E., Fijnheer, R., Geuze, H. J., & Sixma, J. J. (1999). Activated platelets release two types of membrane vesicles: microvesicles by surface shedding and exosomes derived from exocytosis of multivesicular bodies and alpha-granules. *Blood, 94*, 3791–3799.
49. Trajkovic, K., Hsu, C., Chiantia, S., Rajendran, L., Wenzel, D., Wieland, F., et al. (2008). Ceramide triggers budding of exosome vesicles into multivesicular endosomes. *Science, 319*, 1244–1247.
50. Balkay, L., Marian, T., Emri, M., Krasznai, Z., & Tron, L. (1997). Flow cytometric determination of intracellular free potassium concentration. *Cytometry, 28*, 42–49.
51. Schubert, U., Ferrer-Montiel, A. V., Oblatt-Montal, M., Henklein, P., Strebel, K., & Montal, M. (1996). Identification of an ion channel activity of the Vpu transmembrane domain and its involvement in the regulation of virus release from HIV-1-infected cells. *FEBS Letters, 398*, 12–18.
52. Hille, B. (2001). *Ion channels of excitable membranes*. Sunderland: Sinauer.
53. Walz, D., Teissie, J., & Milazzo, G. (2004). *Bioelectrochemistry of membranes*. Basel; Boston: Birkhäuser Verlag.
54. Yu, S. P. (2003). Regulation and critical role of potassium homeostasis in apoptosis. *Progress in Neurobiology, 70*, 363–386.
55. Akari, H., Bour, S., Kao, S., Adachi, A., & Strebel, K. (2001). The human immunodeficiency virus type 1 accessory protein Vpu induces apoptosis by suppressing the nuclear factor kappaB-dependent expression of antiapoptotic factors. *Journal of Experimental Medicine, 194*, 1299–1311.
56. Liu, C., Cotten, J. F., Schuyler, J. A., Fahlman, C. S., Au, J. D., Bickler, P. E., et al. (2005). Protective effects of TASK-3 (KCNK9) and related 2P K channels during cellular stress. *Brain Research, 1031*, 164–173.
57. Lauritzen, I., Zanzouri, M., Honore, E., Duprat, F., Ehrengruber, M. U., Lazdunski, M., et al. (2003). K+-dependent cerebellar granule neuron apoptosis. Role of task leak K+ channels. *Journal of Biological Chemistry, 278*, 32068–32076.
58. Lee, Y. H., Schwartz, M. D., & Panganiban, A. T. (1997). The HIV-1 matrix domain of Gag is required for Vpu responsiveness during particle release. *Virology, 237*, 46–55.